

Selective Heating of Cutaneous Human Tumors at 27.12 MHz

PETER P. ANTICH, N. TOKITA, J. H. KIM, AND E. W. HAHN

Abstract—Data obtained on superficial lesions in different sites and for different patients show that it is possible to correlate average values of the temperature and of the absorbed power density. For healthy tissues, the correlation appears to be defined to within 1°C. For tumor tissues, on the other hand, minimum values of the temperature appear to be predictable. This result indicates that hyperthermic dosimetry is feasible.

Furthermore, a differential temperature phenomenon is observed, in which a localized absorbed power distribution induces higher temperatures in tumors than in the surrounding healthy tissues. This observation, if confirmed with larger statistics and for tumors at a depth, appears to indicate that tumor-killing temperatures can be induced with the heating method employed while simultaneously sparing the surrounding healthy tissues.

I. INTRODUCTION

SINCE FEBRUARY 1975, patients with malignant cutaneous lesions have been treated with radiation and/or hyperthermia in an experimental clinical trial at Memorial Sloan-Kettering Cancer Center. The rationale [1] and preliminary results of this trial have been reported elsewhere [2]. The hyperthermic treatment initially involved the use of a constant temperature water bath for the treatment of tumors of the limbs. In July 1976, an inductive method of radio-frequency (RF) heating at 27.12 MHz was introduced.

We discuss here some aspects of the *in vivo* dosimetry of hyperthermia with the RF method. We present the results of preliminary study on twelve patients and, on the limited statistics thus obtained, we find that it is possible to correlate temperature and absorbed power. Furthermore, we present and discuss our evidence for a temperature differential between tumor and normal tissue.

II. MATERIALS AND METHODS

The heating unit used in this trial was loaned to us by International Medical Electronics, Limited. It is a modified diathermy unit which employs a "pancake" coil to induce the patients with up to 30 W of electromagnetic power at 27.12 MHz. Similar units have been used for physical therapy and are described in the literature [3]. The distribution of absorbed power was measured in a homogeneous phantom. The phantom material was a nor-

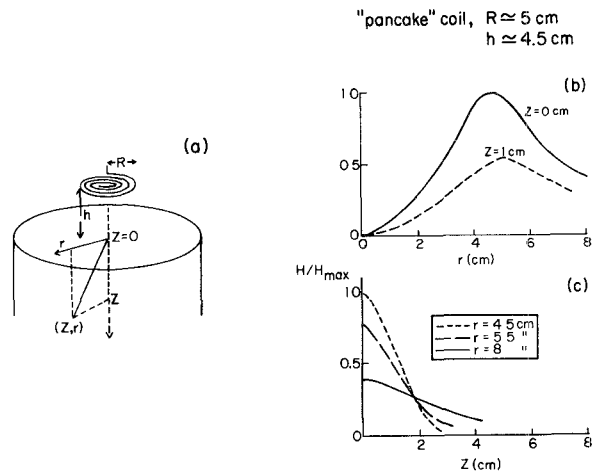


Fig. 1. (a) Schematic representation of the heating method. A three-turn pancake coil of outer radius R heats a cylindrical homogeneous phantom, at a minimum distance h . The coordinate Z (depth from surface of phantom) and r (radial distance from axis of coil) identify points within the phantom. (b) Radial dependence of the relative heat H/H_{\max} at the surface and at a depth of 1 cm. H is the heat induced in phantom by absorption of energy produced by currents circulating in the coil. H_{\max} is the absolute maximum of H in phantom. (c) Depth dependence of the relative heating at three different radial distances.

mal saline solution, gelled and kept in an insulated container opened at the top to permit the insertion of thermocouple arrays. Fig. 1(a) shows the experimental arrangement. The applicator is represented by a three-turn spiral of outer radius ≈ 5 cm. The applicator was kept parallel to, and at a distance of 4.5 cm from, the surface of the phantom. Due to the (approximate) cylindrical symmetry of the absorbed power distribution, only its radial r and depth Z dependence must be analyzed; our choice of coordinates is shown in Fig. 1(a). Hand-drawn curves through the data are shown in Figs. 1(b) and (c), which display the absorbed power H normalized to its absolute maximum value H_{\max} . The distribution of absorbed power has annular peaks at radial distances approximately equal to the outer radius of the coil. The absolute maximum is at zero depth. The absorbed power falls off almost linearly with depth, the slightly negative curvature observed at small depths being due to heat losses from the surface to the environment.

In the clinical condition where surfaces are curved and tissues are electrically inhomogeneous, the prediction of the distribution of heat is a complex problem. However, the distributions observed by us have always had a (de-

Manuscript received September 8, 1977; revised April 5, 1978.

P. P. Antich is with the Mount Sinai School of Medicine, New York, NY 10029.

N. Tokita, J. H. Kim, and E. W. Hahn are with the Memorial Sloan-Kettering Cancer Center, New York, NY 10021.

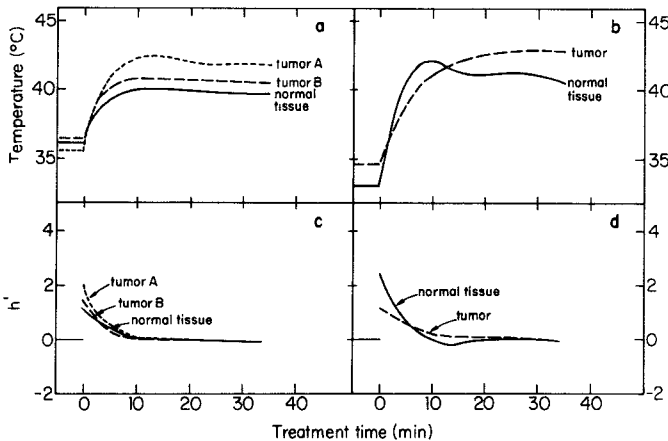


Fig. 2. (a) and (b) Thermal history of two different patients under constant applied power; see text for details. (c) and (d) Time dependence of the rate of temperature h' (2). The discontinuity at $t=0$ may be assumed to be a measure of the absorbed power.

formed) toroidal shape [3] with relative gradients of ≈ 20 percent per centimeter radially and ≈ 30 percent per centimeter of depth.

The measurement of temperature *in vivo* (informed consent was obtained from patients participating in this clinical trial) were made with needle probes (29 gauge) at 2–4 fixed points in each patient, at a distance of 4–6 cm from the applicator's axis, in normal tissue and in tumor, respectively. The fixed points were assured by the insertion of nylon cannulae into the tumor and into adjacent normal tissues, prior to treatment. The thermocouple probes were inserted through these cannulae before heating and during treatment when the RF field was turned off repeatedly but temporarily. The probes were calibrated against an NBS calibrated thermometer. The reading and recording of temperatures were made in a time interval of 5–15 s after turning the RF unit off; all temperatures were then brought to the same nominal time, ≈ 10 s after switchoff. To this end, in a two-probe measurement, the first probe was read at $t=5$ s, the second at $t=10$ s, and then the first again at $t=15$ s; the two readings recorded for the first probe were then averaged. Extrapolating to $t=0$ was found impracticable, but clearly these conventions lead to an underestimate of the actual temperatures which, for different cases, may vary between 0.2 and 0.6°C. The results of two measurements, which were made while keeping the RF unit's output and position constant, are shown in Fig. 2. In Fig. 2(a), the temperature of normal tissue attained a maximum of $\approx 40^\circ\text{C}$ after 13.5 min and then remained approximately constant during the entire treatment; the temperatures measured in tumor were higher but displayed a similar behavior. In Fig. 2(b), the normal tissue temperature reached a maximum value of 42.2°C at 10 min and then decreased (with a second smaller maximum at ≈ 25 min) while the temperature of the tumor increased continuously.

The two cases are representative of the variety of conditions found experimentally; they can be quantitatively

described as follows. In the interaction between applied energy and tissue, heat is locally produced. The thermal properties of the involved and neighboring tissues and fluids, together with the challenged thermoregulatory mechanisms, alter the resulting thermal levels by heat production and transport phenomena. Idealized thermal models may be constructed to describe the situation found in a living organism [4]. These models can be formulated in terms of the heat production and transport equation

$$\rho c \frac{\partial T(\vec{r}, t)}{\partial t} = k \Delta^2 T(\vec{r}, t) + h_{\text{abs}}(\vec{r}, t) + h_m(\vec{r}, t) + h_b(\vec{r}, t). \quad (1)$$

The temperature $T(\vec{r}, t)$ measured in °C at the point \vec{r} at the instant t , varies with time at the rate $\partial T / \partial t$ proportionally to the divergence of the spacial gradient of T at that point and to the sum of the powers per unit volume h , expressed in $\text{cal} \cdot \text{m}^{-3} \text{s}^{-1}$. Here, h_{abs} is the rate at which energy is absorbed, h_m is the rate at which energy is produced metabolically, and h_b is the rate of energy convection by blood flow to a unit volume at the given point and instant. The tissue properties are summarized by the density ρ ($\text{kg} \cdot \text{m}^{-3}$), by the specific heat c ($\text{cal} (\text{°C})^{-1} \text{kg}^{-1}$) and by the thermal conductivity k ($\text{cal} \cdot \text{m}^{-1} \text{s}^{-1}$).

A "treatment plan" necessarily requires some knowledge of each of the terms in (1). This study had, as one of its goals, that of forming a data base for the condition of neighboring tumor and normal tissues, which may be expected to respond differently to thermal stimuli.

For comparison with experimental results, we simplify (1) by writing

$$\frac{\partial T}{\partial t} = h' = \tilde{h}_{\text{abs}} - h'' \quad (2)$$

where $\tilde{h}_{\text{abs}} = 60h_{\text{abs}}/\rho c$ and the heat transport, the metabolic, and the blood-flow terms are lumped together into h'' ; h' , \tilde{h}_{abs} , and h'' have units of °C/min, thus of a rate of change of temperature. If now \tilde{h}_{abs} is changed abruptly from \tilde{h}_{abs}^1 to \tilde{h}_{abs}^2 , $\partial T / \partial t$ will show a discontinuous jump of magnitude

$$\frac{\delta(\partial T)}{\partial t} = \tilde{h}_{\text{abs}}^2 - \tilde{h}_{\text{abs}}^1 \quad (3)$$

and the analysis assumes that any discontinuity in $\partial T / \partial t$ experimentally observed is described by (3).

The temperature history obtained by measuring temperatures at a fixed point at predetermined time intervals contains information about \tilde{h}_{abs} , knowledge of the tissue parameters ρ and c (1) further allows the direct measurement of the absorbed power density h_{abs} .

III. RESULTS

We now turn to the application of these concepts to the data. Figs. 2(c) and (d) display the time dependence of h' (2) obtained from the data of Figs. 2(a) and (b) by differentiation. During the entire treatment, the applied radiation and the position of the applicator with respect to the treated area were kept constant. In agreement with this constancy, discontinuities are observed only at the

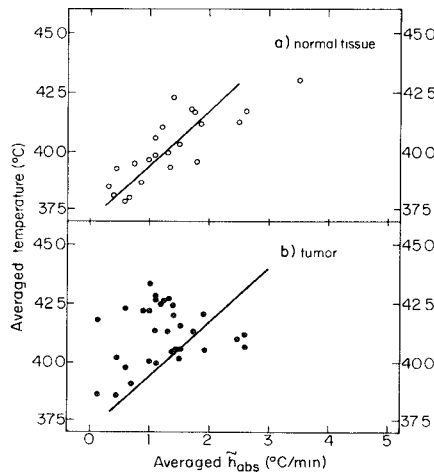


Fig. 3. Averaged temperatures at different points in normal tissue and tumor, as functions of the averaged rates of change of temperature due to absorbed power \tilde{h}_{abs} (2). The average values are calculated at fixed points over an interval of time starting at 7.5 min after the beginning of the treatment and extending to the end of it (see text). The line segment is drawn as a guide to the eye and represents a linear fit to the normal tissue data.

time when power is first applied ($t=0$) and their value is attributed to \tilde{h}_{abs} . Assuming that \tilde{h}_{abs} remains constant—at least in a first approximation—the continuous decrease of h' may be then attributed to an increase of h'' from an initial value of 0 (at thermal equilibrium) to an asymptotic value equal to \tilde{h}_{abs} . The asymptotic value is reached either monotonically, as in Fig. 2(c) and for the tumor of Fig. 2(d), or in a damped oscillation, with a change of sign, as in the curve for normal tissue of Fig. 2(d). In cases where the external power is not constant, \tilde{h}_{abs} will change correspondingly during the treatment. Making use of (3), \tilde{h}_{abs} may, however, be computed at all times.

An important practical question is then: can temperature be correlated with the rate of energy absorption? To investigate this question, we first consider the value of the temperature and of the rate of change of temperature \tilde{h}_{abs} , both averaged over the time interval starting at $t=7.5$ min and ending at the end of the treatment. This is admittedly an arbitrary definition but (as shown, e.g., in Fig. 2) it corresponds to an interval of time during which fluctuations are generally small. Some preliminary results are shown in Fig. 3, for normal tissues (a) and tumors (b). The data was obtained from 20 treatments of 12 different patients; the temperatures were measured at one or more points in normal tissue and in tumor, respectively. While the statistical significance of the data are small, the two distributions are obviously different; the data point for normal tissue cluster more closely about the straight line shown. The difference is more clearly displayed in Fig. 4, where the average temperature differential is plotted against the \tilde{h}_{abs} differential between tumor and surrounding tissue.

This difference in average quantities reflects the difference between the temperature histories during the treatment. To illustrate this difference, we show in Fig. 5 the

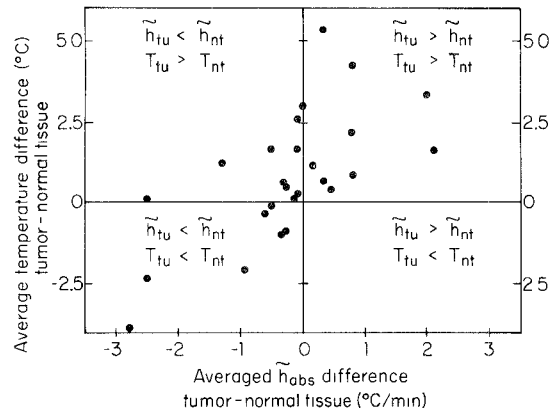


Fig. 4. Difference between the averaged temperature in tumor and surrounding normal tissues, as a function of the difference between the average \tilde{h}_{abs} . The four quadrants are explicitly labeled, and it may be seen that the two distributions of \tilde{h}_{abs} coincide, while the temperature in tumor is higher than in normal tissue in two thirds of the cases.

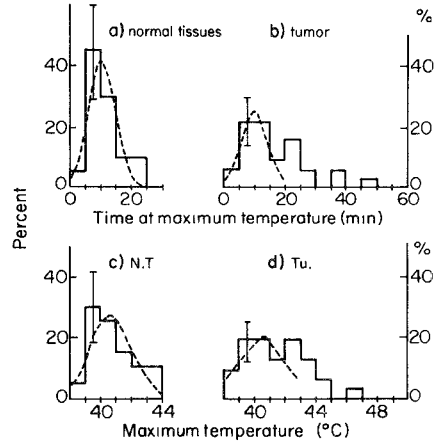


Fig. 5. (a) and (b) Normalized histogram of the time at which the (first) maximum of the temperature is reached in normal tissue and in tumor. The curve is a Gaussian fit to the normal tissue data with a mean value of 10.8 min and a standard deviation of 4.4 min. The curve is renormalized and superimposed on the tumor data as a guide to the eye. (c) and (d) Normalized histogram of the maximum temperatures reached in normal tissue and in tumor. The Gaussian fit to the normal tissue data has a mean of 40.6°C and a standard deviation of 1.4°C.

distributions of the time at which the temperature reaches its maximum and of the value of the maximum, for normal tissues and tumors, respectively. The curves are Gaussian fits to the normal tissue distributions, which are then renormalized and superimposed on the tumor distributions for comparison. The tumor distributions are broader and display tails for temperatures and times larger than those of normal tissues.

IV. DISCUSSION AND CONCLUSIONS

As shown in Fig. 4, while \tilde{h}_{abs} is greater in tumor than in normal tissue in half the cases, the temperature is greater in tumor in two thirds of the cases; thus some mechanism must play a role in enhancing temperature differentials between normal tissues and tumors.

In one such mechanism proposed in view of its known large effect in the cooling of normal tissues [5], the ther-

moregulatory system would act directly on normal tissues alone, while it would not be an integral part of the lesions. Thus as long as the rate of heat production in a tumor was larger than the rate of heat exchange with the surrounding cooled tissues, the tumor temperature would increase. Therefore, in this hypothesis, the cooling term h'' of (2) would equilibrate (and/or overcompensate) the power absorption term \tilde{h}_{abs} more quickly in normal tissues than in tumors. As when h'' equals \tilde{h}_{abs} , the temperature reaches its maximum; to study this effect we may consider this value and the time at which it is attained. The data of Fig. 5 show that indeed the time at maximum has a rather narrow distribution centered at ~ 10 min for normal tissue, while it has a broader tail reaching ~ 30 min for tumors. The distribution of the maximum temperatures observed in tumor is also broader, and favors higher values than those of normal tissue. These observations are in agreement with the proposed thermoregulatory mechanism. *A priori*, a second mechanism could be present, either alternative or complementary to the one just described. For this mechanism, the thermal properties of tumors would differ from those of the surrounding normal tissues. Let us first consider the thermal conductivity k of (1). The validity of the hypothesis that the observed differences are due to this property would imply that the thermal conductivity of tumors is appreciably larger than that of the normal tissues investigated. In this case, the transport of heat away from the lesion would be more difficult than in the other direction, with effects qualitatively similar to those of the thermoregulatory mechanism considered above.

Secondly, we must consider the specific heat c , or the product ρc of (1). If this had, in tumors, a range of values mainly larger than in normal tissues, the differences shown in Figs. 3 and 4 might disappear when plotting average temperatures against average absorbed power densities. To illustrate this point, Table I shows the average value and standard deviation of the temperature rise distribution in tumor and normal tissue, and the corresponding values for the absorbed power density under different assumptions. Quantitatively, as indicated in Table I, the validity of this mechanism appears difficult to substantiate.

We, therefore, conclude that the selective heating effect displayed in Figs. 3 and 4 are real and not due to a wrong choice of physical variables. This observation indicates that it is possible to induce localized hyperthermia by localized inductive heating, at least in the case of superfi-

TABLE I
MEAN VALUE $\langle h_{abs} \rangle_{av}$ AND STANDARD DEVIATION $\sigma(h_{abs})$ OF THE ABSORBED POWER DENSITY CORRESPONDING TO THE VALUES OF $\langle h_{abs} \rangle_{av}$ AND $\sigma(h_{abs})$ EXPERIMENTALLY OBSERVED IN NORMAL AND IN TUMOR TISSUE, UNDER DIFFERENT ASSUMPTIONS ON THEIR NATURE. THE TISSUE DENSITY AND SPECIFIC HEAT VALUES ARE TAKEN FROM GUY [3]. THEY CORRESPOND TO (a) FAT (TISSUE POOR IN WATER CONTENT), (b) MUSCLE (TISSUE RICH IN WATER CONTENT) AND (c) BLOOD

Tissue	Assumed Value of ρc (Cal/ $^{\circ}\text{C}\text{m}^3$)	$\langle \tilde{h}_{abs} \rangle_{av}$ ($^{\circ}\text{C}/\text{min}$)	$\sigma(\tilde{h}_{abs})$ ($^{\circ}\text{C}/\text{min}$)	$\langle h_{abs} \rangle_{av}$ (kW/m^3)	$\sigma(h_{abs})$ (kW/m^3)
Normal	0.51 a	1.35	0.79	48	28
	0.89 b			84	49
	0.51 a			43	22
Tumor	0.89 b	1.24	0.62	77	38
	0.99 c			86	43

cial tumors. Moreover, we have observed a definite correlation between absorbed power and average temperature. This result indicates that a dosimetry based on the measurement of absorbed power is capable of giving a degree of description of the ensuing thermal field. In this description, normal tissue temperatures would be well defined while for tumors, a range of temperatures would be obtained with a predictable minimum value.

Further experimentation is under way with the aim of quantifying these conclusions with larger statistics and on a wider range of absorbed powers and temperatures. It is also planned to study the effect of the heat transport term $k\nabla^2T$ and of the correlations between thermoregulatory response and temperature differentials. Knowledge of these terms may allow a more precise description of temperature distributions in tumors and in normal tissue and may be of great value in the planning of hyperthermal treatments.

REFERENCES

- [1] E. W. Hahn and J. H. Kim, "Hyperthermia in cancer research," *Clinical Bull.*, vol. 5, pp. 165-167, 1975.
- [2] J. H. Kim, E. W. Hahn, N. Tokita, and L. Nisce, "Local tumor hyperthermia in combination with radiation therapy. I. Malignant cutaneous lesions," *Cancer*, vol. 40, pp. 161-169, 1978.
- [3] A. W. Guy, "Physical aspects of the electromagnetic heating of tissue volume, in *Proc. Int. Symp. on Cancer Therapy by Hyperthermia and Radiation*, Washington, DC, pp. 183-205, 1975.
- [4] H. F. Bowman, E. G. Cravalho, and M. Woods, "Theory, measurement, and application of thermal properties of biomaterials," *Annu. Rev. Biophys. Bioeng.*, vol. 4, pp. 43-80, 1975.
- [5] J. A. J. Stolwijk, "Physiological response to whole body and regional hyperthermia," in *Proc. Int. Symp. Cancer Therapy by Hyperthermia and Radiation*, Washington, DC, ACR, pp. 163-167, 1975.